coatings

MDPI

*Article*

# Development and Characterization of Films for Food Application Incorporating Porphyran Extracted from *Porphyra dioica*

**Marco Teles [1], Pedro Adão [2], Clélia Afonso [1], Raul Bernardino [1,3], Mafalda Guedes [4,5], Ricardo Baptista [4,6] and Susana Bernardino [1,*]**

1 MARE, School of Tourism and Maritime Technology, Polytechnic of Leiria, 2520-641 Peniche, Portugal; marco98teles@gmail.com (M.T.); clelia@ipleiria.pt (C.A.); raul.bernardino@ipleiria.pt (R.B.)
2 MARE, Polytechnic of Leiria, 2520-641 Peniche, Portugal; pedro.adao@ipleiria.pt
3 Laboratory of Separation and Reaction Engineering-Laboratory of Catalysis and Materials (LSRE-LCM), School of Tourism and Maritime Technology, (ESTM), Polytechnic of Leiria, 2411-901 Leiria, Portugal
4 CDP2T, Setúbal School of Technology, Polytechnic of Setúbal, 2910-761 Setúbal, Portugal; mafalda.guedes@estsetubal.ips.pt (M.G.); ricardo.baptista@estsetubal.ips.pt (R.B.)
5 CEFEMA, Instituto Superior Técnico, ULisboa, Av. Rovisco Pais 1, 1000-001 Lisboa, Portugal
6 IDMEC, Instituto Superior Técnico, ULisboa, Av. Rovisco Pais 1, 1000-001 Lisboa, Portugal
* Correspondence: susana.bernardino@ipleiria.pt

**Abstract:** Non-biodegradable plastic is one of the biggest environmental problems of our lifetime and, considering the present societal needs, it will get worse. Consequently, there is an urgent need to develop sustainable and renewable alternatives to plastic, such as plastic-like materials obtained from biodegradable polymers, namely sulfated polysaccharides, considered one of the most viable alternatives. There is also a need to obtain these materials in an environmentally and economically sustainable way. The hereby developed process of obtaining film-forming solutions from semi-refined porphyran (PorphSR) uses a green solvent (hot water) with a high extraction yield of semi-refined porphyran (26.66 ± 0.27%) in a reproducible way and with low levels of contaminants. The obtained semi-refined porphyran showed good antioxidant potential in all tests performed: HPSA (Δ0.066 ± 0.002), DPPH (2.23 ± 0.78%), FRAP (0.420 ± 0.014 eq. ascorbic acid μg $mg^{-1}$ of extract) and ABTS (20.46 ± 0.90%). After being cast into films, the most notable antioxidant properties were those of the semi-refined porphyran in the DPPH, FRAP and ABTS assays and of the pectin, (PorphSR_PcT and PorphSR_PcT_Gly) in the HPSA assay. Morphologically, the films showed relatively homogeneous and low roughness surfaces. It is concluded that the described method to obtain semi-refined porphyran is feasible and reproducible, and that the developed films, mainly PorfP2_PcT_Gly, proved to be a potential candidate for non-biodegradable plastic substitutes.

**Keywords:** biodegradable plastic; composite materials; polysaccharides; porphyran; *Porphyra dioica*



**Citation:** Teles, M.; Adão, P.; Afonso, C.; Bernardino, R.; Guedes, M.; Baptista, R.; Bernardino, S. Development and Characterization of Films for Food Application Incorporating Porphyran Extracted from *Porphyra dioica*. *Coatings* **2022**, *12*, 148. https://doi.org/10.3390/coatings12020148

Academic Editor: Shih-Chen Shi

Received: 23 December 2021
Accepted: 17 January 2022
Published: 26 January 2022



## 1. Introduction

Petroleum-derived plastic is a virtually non-degradable anthropogenic compound, and its residues constitute one of the biggest environmental problems of our time [1]. It is non-biodegradable due to its long-chain polymeric structure, lacking a functional group susceptible to microbial degradation, high molecular weight, hydrophobicity and crystallinity [2].

Due to its diverse applications, there has been a 20-fold increase in production over five decades since 1964, reaching 335 million tons in 2015 [2], with a forecast of doubling by 2038 and nearly quadrupling by 2050 [3]. The largest consumption sector is packaging, with special relevance to the food industry [4].

Plastic debris is a threat to marine life and a growing environmental problem that occurs on a global scale [5,6]. The main threats of macroplastics arise from ingestion, leading to the obstruction of the digestive and/or respiratory systems, and entanglement in plastic

debris, such as synthetic lines and ropes, reducing or impairing the locomotion and growth of organisms [7]. Additionally, microplastics, microscopic fragments of plastic, can be introduced into the food chain through ingestion, affecting all trophic levels, including non-marine organisms; its toxicity can trigger pathologies [8], and, by direct contact, they can cause rashes and skin irritation [9,10] in many living organisms, including humans [11,12].

Presently, plastic plays a prominent role as a starting material, being present in all types of industries and everyday processes due to its inherent physical and mechanical properties and its low production cost. However, its durability, origin and interactions with organisms, above mentioned, make plastic a global threat to the ecosystems, and the development of alternatives that maintain all the sought-after properties but greatly reduce the environmental impact is direly needed [13]. Biodegradable plastics are the main candidates to address this problem, namely polymers of biological or synthetic origin that can be degraded by organisms into components that can be reintroduced into ecosystems, ideally without causing damage [14]. These biodegradable plastics can form films, independent solid structures formed by polymeric matrices, that can be used in the packaging of foods [15]. The mechanical properties of these films are defined by the starting raw materials, the chosen synthetic process and the additives used [16].

Packaging must establish a physical protective barrier against the main external factors that accelerate food degradation, such as chemical agents, gases such as oxygen, carbon dioxide, moisture level or other compounds, or physical events such as impacts and vibrations during the transport, and protection against biological agents such as microorganisms and insects [17,18]. One way to ensure the suitability of the packaging is to evaluate the change in the food's sensory parameters, namely the taste, over time, as this properties should not change after packaging [19].

The required physical characteristics of the packaging material, such as rigidity, flexibility or color, are defined by the food product for which it is intended and by the distribution circuit to which it will be submitted to [20]. The composition must therefore be adjusted to each product and its intended distribution circuit in order to obtain a material with the desired packaging characteristics [21]. Additionally, it may contain favorable bioactivities such as antioxidant [22] and antimicrobial [23] properties, leading to an active packaging material.

The perfect film must not contain toxic and/or allergenic compounds in its composition; it must regulate the water migration from food and the gas exchange; it must avoid the absorption or loss of compounds that interfere with the aroma, flavor or nutritional properties; it must provide biochemical and microbial stability and, at the same time, protect against microbial contamination and proliferation, be aesthetically pleasing and be able to incorporate desirable additives [21]. Films are usually formed by direct casting on flat surfaces followed by drying, namely in an oven or a drying tunnel [24]. Films can be cast from composite materials, a mixture of two or more materials, to obtain a final film with improved physical, chemical and/or bioactive characteristics [25]. The film matrix can present homogeneous or heterogeneous morphology, depending on the compatibility of the components and the constitution of the film [26,27].

Sulfated polysaccharides are a complex group of anionic macromolecules [28], which can be extracted and isolated from algae using hot water, acid or dilute base, using large volumes of solvent [29]. Due to their physical, chemical and biomechanical properties, their bioactive characteristics and their biocompatibility, sulfated polysaccharides are already used in various industries, such as pharmaceutical, cosmetic, food and medical equipment, among others [30,31]. Porphyran is a sulfated polysaccharide extracted from algae of the genus *Porphyra* and is one of the most studied agarans [32,33].

*Porphyra dioica* J. Brodie and L. M. Irvine 1997 is a species native to the North Atlantic coast that occurs from the northeast coast of the United States of America to the northwest of Portugal in the intertidal zone [34,35]. It grows in a relatively wide range of conditions, such as temperature, photoperiod and light intensity [36], and due to its fast growth and high absorption of nitrates, phosphates and carbon dioxide, this species has a high

potential for bioremediation, allowing its use in multitrophic culture systems [37,38] with fast biomass production at a low cost [39].

Structurally, porphyran (Figure 1) consists of (1,3-β) D-galactose residues alternating with (1,4-α) L-galactose-6-sulfate or 3,6- anhydrous-α-L-galactose, and substitutions with sulfate ester residues may occur [40]. Sulfate groups represent 10–11% of dry biomass weight [41].

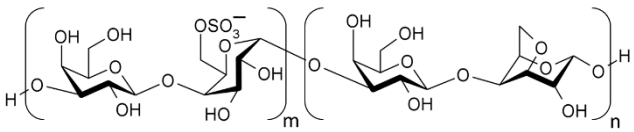


**Figure 1.** Idealized structure of porphyran, depicting the main repeating units.

Like alginate and carrageenan, porphyran is an anionic hydrocolloid, from which it is possible to obtain films from filmogenic solutions using water as a solvent; however, according to the published results, its application in food packaging is still under-exploited, as shown by the limited number of reports in the literature. As stated, the present study develops a new method of porphyran extraction from *Porphyra dioica*, using a small volume of water, with a high yield and ease of scaling up, resulting in biodegradable porphyran-based films with antioxidants properties that can be used in dry food with high lipid content packaging, such as chocolate cereals, in which lipid oxidation and water absorption are the main factors responsible for shelf life reduction.

## 2. Materials and Methods

### *2.1. Extraction of Semi-Refined Porphyran (PorphSR)*

The extractions were performed using a Soxhlet extractor and a heating mantle Fibroman-c (J.P Selecta SA, Abrera, Barcelona, Spain).

About 15 g of dry powdered *Porphyra dioica* (≤0.25 mm) (ALGAplus, Ílhavo, Aveiro, Portugal) were distributed on three sheets of absorbent laboratory paper and rolled up to form a cartridge. These were moistened and placed in the Soxhlet extractor. In a 1000 mL collector, 500 mL of distilled water and ceramic chips were placed. The extraction solvent was heated to boiling point with a heating mantle set to about 200 °C at 7-h intervals, with rest periods overnight. After this rest period, the contents of the collector were recovered, and this process was repeated for two days. The contents of the collector corresponding to the first 1-h extraction were discarded.

The contents recovered from the collector were heated to approximately 100 °C and filtered with a 90 mm quantitative 2240 filter paper (Filter-Lab, Laval, QC, Canada) under vacuum and evaporated in a rotary evaporator at 60 °C, 260 rpm and 20 mbar until a thick, very viscous mass is formed. Then, 400 mL of 90% isopropanol was added, allowed to precipitate, decanted, and 200 mL of 99.9% isopropanol were added (Carlo Erba, Milan, Italy). The contents were fragmented in a blender and filtered with a 90 mm quantitative 2240 paper filter under vacuum. The content present in the filter was washed with the addition of small volumes of isopropanol, recovered and placed in an oven at 60 °C for 24 h to remove all solvent residues.

### *2.2. p-Benzoquinone Assay*

Protein quantification was performed using the *p*-Benzoquinone method, adapted from Amin and El-Didamony (2003) [42]. The reaction was mediated by phosphate buffer at pH 9.2, composed of anhydrous monobasic sodium phosphate (Amresco, Solon, OH, USA) and pH adjusted with NaOH. A solution of *p*-benzoquinone (Sigma-Aldrich, St. Louis, MO, USA) to 1 mg·mL$^{-1}$ (*p*-BQ) in phosphate buffer at pH 9.2. The external standard was obtained by diluting a solution of an amino acid, in this case L-alanine (PanReac AppliChem, Castellar del Vallès, Barcelona, Spain), to 0.3 mg·mL$^{-1}$ in phosphate buffer at pH 9.2. The samples were prepared in phosphate buffer at pH 9.2 at a concentration of 0.6 mg·mL$^{-1}$. The HCl (VWR Chemicals, Radnor, PA, USA) solution 2.5 M was prepared in ethanol 96%. The

calibration concentrations were 30–5 μg·mL$^{-1}$ and 0 μg·mL$^{-1}$. Samples were prepared at an initial concentration of 0.6 mg·mL$^{-1}$. Then, 1 mL of *p*-BQ was added to 2 mL of the sample or standard solution that immediately after was kept in a 50 °C bath for 15 min. Finally, 3 mL of 2.5 M HCl were then added, and the absorbance at 467 nm was read. All measurements were performed in three independent trials and triplicate. Sample results were interpreted based on the L-alanine standard calibration curve.

### *2.3. Phenol-Sulfuric Acid Method*

The quantification of galactose was performed using the phenol-sulfuric acid method, adapted from Rao and Pattabiraman (1989) [43]. The initial concentration of the phenol solution, 10 mg·mL$^{-1}$, was prepared from phenol crystals (Fisher Scientific, Waltham, MA, USA). The external standard was obtained throughout dilutions of D-galactose (VWR, Radnor, PA, USA) 0.6 mg·mL$^{-1}$ in distilled water. Samples were prepared in distilled water at 0.6 mg·mL$^{-1}$. The calibration concentrations were 45–7.5 μg·mL$^{-1}$ and 0 μg·mL$^{-1}$. To 0.6 mL of samples or of standard solution, 1.8 mL of 95% sulfuric acid (VWR, Radnor, PA, USA) and 0.6 mL of phenol solution were added, and then, after the exothermic reaction ended, 5 mL of distilled water were added, and the resulting solution was read at 495 nm absorbance. The 495 nm absorbance of the samples was also measured with $H_2SO_4$ and distilled water in the proportions described, replacing the phenol solution with distilled water, and this absorbance was subtracted from the previous values. All measurements were performed in three independent trials and in quadruplicate. Sample results were interpreted based on the D-galactose standard calibration curve.

### *2.4. Quantification of Total Phenols (QTP)*

The quantification of total phenols (QTP) was determined with the Folin–Ciocalteu (F-C) reagent (AppliChem, Darmstadt, Germany) based on the method by Fu et al. (2010) [44]. Calibration was obtained using a solution of gallic acid (Merck KGaA, Darmstadt, Germany) at 0.1 mg·mL$^{-1}$ with the following concentrations: 6–1 μg·mL$^{-1}$ and 0 μg·mL$^{-1}$. Sample solutions at 2 mg·mL$^{-1}$ in distilled water were prepared. The F-C reagent was diluted 1:10 in water, and the sodium carbonate solution (Scharlau, Sentmenat, Barcelona, Spain) was saturated to 75 mg·mL$^{-1}$. The analysis was performed by mixing 0.5 mL of the sample or standard solution and 2.5 mL of diluted FC reagent, followed by the addition of 2 mL of sodium carbonate to the mixture after 4 min. The reaction allowed to run for 2 h at room temperature. After this period, the absorbance at 760 nm was read. All measurements were performed in three independent trials and in triplicate. Sample results were interpreted based on the gallic acid standard calibration curve.

### *2.5. Hydrogen Peroxide Scavenging Assay (HPSA)*

The hydrogen peroxide scavenging assay was adapted from Bektaşoğlu et al. (2008) [45]. A solution of sodium iron(III) ethylenediaminetetraacetate (NaFeEDTA) and methyl red was prepared by dissolving 0.251 g of NaFeEDTA, formed by the addition of ethylenediaminetetraacetic acid disodium salt dihydrate (VWR Chemicals, Radnor, PA, USA) and chloride of Iron (III) (Labkem, Barcelona, Spain) in a saturated solution of methyl red (Ika, Radnor, PA, USA), 12 mg in 500 mL of distilled water and 0.2 mL of acetic acid (VWR Chemicals, Radnor, PA, USA), which was filtered with a quantitative paper filter 2240.

The preparation of the samples for analysis consisted of mixing 1 mL of the polysaccharide stock solution at 0.6 mg·mL$^{-1}$ and 1.8 mL of the NaFeEDTA/methyl red/acetic acid solution with 0.2 mL of 30% hydrogen peroxide (Chem-Lab, Zedelgem, Belgium). The sample was homogenized, and the absorbance at 524 nm was measured immediately at t = 0 min and t = 10 min. The change in absorbance after 10 min was determined by subtracting the referred values. All measurements were performed in three independent trials and in quadruplicate.

### 2.6. DPPH (2,2-Diphenyl-1-picrylhydrazyl) Radical Scavenging Activity

The DPPH assay was based on Andrade et al. (2018) [46]. The DPPH solution was prepared at 0.142 mg·mL$^{-1}$ in methanol (Chem-Lab, Zedelgem, West Flanders, Belgium). The samples were prepared in distilled water at a concentration of 0.8 mg·mL$^{-1}$. Ascorbic acid calibration concentrations were 2–0.4 µg·mL$^{-1}$ and 0.0 µg·mL$^{-1}$.

Then, 2 mL of DPPH were added to 0.05 mL of samples or standard solution. The reaction took place in the dark at room temperature, and after 30 min the absorbance at 517 nm was read. All measurements were performed in three independent trials and in triplicate. The %Inhibition (mg$^{-1}$ of the sample) was determined using the equation

$$\%\text{Inhibition}\left(\text{mg}^{-1}\text{ of sample}\right) = \frac{\frac{\text{Abs t0min}_{517\text{nm}} - \text{Abs t30min}_{517\text{mn}}}{\text{Abs t0min}_{517\text{nm}}} \times 100}{\text{m}_{\text{Sample}}\text{ mg}} \quad (1)$$

### 2.7. Ferric-Reducing Antioxidant Power (FRAP)

The ferric-reducing antioxidant power assay was adapted from Berker et al. (2007) [47]. In preparing the standard, a solution of ascorbic acid (Villassar de Dalt, Barcelona, Spain) at 0.292 mg·mL$^{-1}$ in distilled water was used. The samples were prepared in distilled water at a concentration of 0.6 mg·mL$^{-1}$.

The calibration concentrations changed from 2.60 µg·mL$^{-1}$ to 0.65 µg·mL$^{-1}$ and 0.00 mg·mL$^{-1}$. The reaction was carried out using 1 mL of samples or standard solution, 1.5 mL of distilled water and 0.5 mL of Fe(1,10-phenanthroline)$_3$Cl$_3$ reagent, (1,10-phenanthroline monohydrate, Sigma-Aldrich, St. Louis, MO, USA, $FeCl_3 \cdot 6H_2O$, Sigma-Aldrich, St. Louis, MO, USA) at 3.3 mM. The reaction took place in the dark at room temperature, and after 30 min, 6 mL of distilled water was added and the absorbance at 510 nm was read. All measurements were performed in three independent trials and in triplicate. Sample results were interpreted based on the ascorbic acid standard calibration curve.

### 2.8. 2,2′-Azinobis-(3-Ethylbenzothiazoline-6-Sulfonic Acid Assay (ABTS)

The ABTS reagent, consisting of 48 mg of 2,2′-azino-bis-(3-ethylbenzothiazoline-6-sulfonic acid) ($C_{18}H_{16}N_4O_6S_4$-$(NH_4)_2$) (Alfa Aesar, Haverhill, MA, USA) and 12.8 mg potassium peroxydisulfate ($K_2S_2O_8$) (Alfa Aesar, Haverhill, MA, USA) in 250 mL of water was prepared and stored for 16 h at room temperature in the dark before use. Calibration was performed using an ascorbic acid solution at 61.2 µg·mL$^{-1}$. The standards were used in concentrations of 6.12–1.02 µg·mL$^{-1}$ and 0.00 µg·mL$^{-1}$. For the samples the concentration was 0.6 mg·mL$^{-1}$.

The reaction medium consisted of 2 mL of ABTS reagent, 2 mL of sample or standard solution and 2 mL of distilled water. The reaction occurred in 1 min and its absorbance spectra from 500 to 850 nm was read immediately after this period; the procedure was modified from Pellegrini et al. (1999) [48]. All measurements were performed in three independent trials and in triplicate. The %Inhibition·mg$^{-1}$ of the sample was determined using the equation

$$\%\text{Inhibition}\left(\text{mg}^{-1}\text{ of sample}\right) = \frac{\frac{\text{Abs t0min}_{734\text{nm}} - \text{Abs t1min}_{734\text{mn}}}{\text{Abs t0min}_{734\text{nm}}} \times 100}{\text{m}_{\text{Sample}}\text{ mg}} \quad (2)$$

### 2.9. Film Formulation

The films were produced by a casting process adapted from (Nieto, 2009) [49]. Filmogenic solutions were developed from the semi-refined porphyrane (PorphSR) described above, sodium carboxymethylcellulose (CMC) (Fluka, Buchs, St. Gallen, Switzerland), food pectin (PcT) (Sosa, Moià, Barcelona, Spain), sodium alginate (AL) (VWR, Radnor, PA, USA), 86–88% glycerol (Scharlau Chemie SA, Sentmenat, Barcelona, Spain) and calcium chloride ($CaCl_2$) (Chem-Lab, Zedelgem, East Flanders, Belgium) in the proportion described in Table 1 and dissolved in distilled water at 100 °C. After complete dissolution the solutions

were filtered with quantitative 2240 paper filter under vacuum, and, as applicable, glycerol was added. After filtration, the filmogenic solution remained for 1–2 h at approximately 100 °C with constant agitation, after which 25 mL of filmogenic solution was applied to the molds of 56.74 $cm^2$ (25 mL, 0.44 $mL \cdot cm^{-2}$). The molds with the solution remained under vacuum for 20–60 min and then were placed in a UF 110 oven (Memmert, Büchenbach, Roth, Germany) at 40 °C and 10% ventilation capacity for 18–20 h. Afterwards the mold was placed on a surface at approximately 60 °C, and the film was removed.

**Table 1.** Composition of film-forming solutions by components, semi-refined porphyran extracted by the Sohxlet method, sodium carboxymethylcellulose (CMC), pectin (PcT), sodium alginate (AL) and glycerol (Gly).

| Film-Forming Solutions (V = 25 mL) | Porph SR (g) | CMC (g) | PcT (g) | AL (g) | Gly (μL) |
|---|---|---|---|---|---|
| PorphSR_ | 0.250 | 0 | 0 | 0 | 0 |
| PorphSR_Gly | 0.250 | 0 | 0 | 0 | 30 |
| PorphSR_CMC | 0.250 | 0.250 | 0 | 0 | 0 |
| PorphSR_CMC_Gly | 0.250 | 0.250 | 0 | 0 | 30 |
| PorphSR_PcT | 0.250 | 0 | 0.250 | 0 | 0 |
| PorphSR_PcT_Gly | 0.250 | 0 | 0.250 | 0 | 30 |
| PorphSR_AL | 0.125 | 0 | 0 | 0.250 | 0 |
| PorphSR_AL_Gly | 0.125 | 0 | 0 | 0.250 | 30 |

### 2.10. Electron Microscopy

The films were analyzed by field emission scanning electron microscopy (FEG-SEM, JSM-7001F, JEOL, Tokyo, Japan). Samples were previously coated with an Au-Pd alloy to avoid an accumulation of electrical charge during observation.

### 2.11. Mechanical Tests

Tensile tests were performed on a universal electromechanical testing machine (INSTRON, 5544, Norwood, MA, USA), equipped with a 100 N load cell (INSTRON) and a video strain gauge (INSTRON, SVE I, Norwood, MA, USA). Tests were carried out until sample fracture with a speed of 1 mm/min. Both the Young's modulus and the sample ultimate tensile stress (UTS) were calculated according to ASTM D638 (Standard Test Method for Tensile Properties of Plastics). At least 3 ($n = 3 \ldots 6$) samples with 15 mm width and 55 mm gauge length (over 95 mm long) were used per film composition. Sample thickness (between 25 and 59 μm) was determined using the Archimedes method.

### 2.12. Sensory Analysis

In the present study, chocolate cereal balls (Dia, Las Rozas, Madrid, Espanha), which have high lipid content as intended, were packaged in the test films (PorphP2_AL_Gly, PorfP2_PcT_Gly e PorfP2_CMC_Gly) and in the control film (polyethylene) for 2 months. The samples were subsequently submitted to a triangular sensory analysis test in which 12 untrained tasters have participated. This was followed by the methodology described by Meilgaard, Carr e Civille (1999) [50]. Each participant was asked to taste sets of 3 samples, two being the same and one different, to determine differences between samples. Six replicates were used with porphyran films per taster with random order and three replicates with the control. All samples were compared with each other and with the control.

### 2.13. Statistical Treatment

Statistical analysis was performed using ANOVA tests with one factor; in the case of statistically significant differences, the Tukey multiple comparison test was performed. The tests have a significance of 5% and were analysed by the GraphPad Prism 8.0.2 software. The graphical representations were made using the GraphPad Prism 8.0.2. Lowercase letters represent statistically significant differences; data with the same letters do not show

statistically significant differences from each other and data that do not contain a letter do not show statistically significant differences with the negative control.

## 3. Results

### *3.1. Extraction Methods*

Table 2 shows the porphyran extraction yield obtained by applying the extraction method developed from *Porphyra dioica* and the main components present. The yield obtained was 26.66% in algae dry weight; the protein content was below the detection limit; the concentration of D-galactose corresponded to 67.74% of the dry weight of the extract, and the presence of phenols was detected in 0.616 gallic acid equivalent $\mu g \cdot mg^{-1}$ of sample.

**Table 2.** Characterization of semi-refined porphyran extracts obtained by the method described.

| | Yield (%) | [Protein] (%) | [D-Galactose] (%) | Total Phenols (Gallic Acid Equivalent $\mu g \cdot mg^{-1}$ of Sample) |
|---|---|---|---|---|
| PorphSR | 26.66 ± 0.27 | * ND | 67.74 ± 4.13 | 0.616 ± 0.027 |

* ND–Not Detected. The presented values are mean values ± standard deviation of 3 independent assays in triplicate or quadriplicate.

### *3.2. Antioxidant Potential*

The antioxidant properties, determined by the described HPSA, DPPH, FRAP and ABTS methods, of the extract, PorphSR, of the remaining components of the films, food pectin (PcT), sodium carboxymethylcellulose (CMC), sodium alginate (AL) and glycerol 86–88% (Gly) and of the films produced (Table 1) are presented in Table 3, with all the samples being compared to a negative control. Lowercase letters represent statistically significant differences; data with the same letters do not show statistically significant differences from each other and data that do not contain a letter do not show statistically significant differences with the negative control.

**Table 3.** Compilation of the antioxidant properties of PorphP2 extract, pectin (PcT), sodium carboxymethylcellulose (CMC), sodium alginate (AL), glycerol 86–88% (Gly) films and developed films. Lowercase letters on data symbolize the statistically significant differences with a significance of 5%.

| | HPSA (ΔAbs a 524 nm) | DPPH (%Inhibition) | FRAP (Ascorbic Acid Equivalent $\mu g \cdot mg^{-1}$ of Sample) | ABTS (%Inhibition) |
|---|---|---|---|---|
| PorphSR | 0.066 ± 0.002 a | 2.23 ± 0.78 a | 0.420 ± 0.014 a | 20.46 ± 0.90 a |
| PcT | 0.019 ± 0.002 b | 1.14 ± 0.28 | −0.009 ± 0.015 | 2.67 ± 0.76 |
| CMC | 0.108 ± 0.009 c | 1.30 ± 1.71 | 0.016 ± 0.011 | 2.20 ± 0.44 |
| AL | 0.113 ± 0.006 c | 1.95 ± 0.69 | 0.038 ± 0.007 | −0.80 ± 0.44 |
| Gly | 0.028 ± 0.001 b | 1.22 ± 0.48 | −0.010 ± 0.005 | 2.76 ± 0.39 |
| PorphSR_PcT | 0.017 ± 0.002 d | −0.25 ± 0.66 | 0.207 ± 0.028 c | 7.51 ± 1.31 c |
| PorphSR_PcT_Gly | 0.028 ± 0.001 e | −0.02 ± 0.71 | 0.168 ± 0.049 c | 6.62 ± 0.41 c |
| PorphSR_CMC | 0.090 ± 0.001 | 0.44 ± 0.10 | 0.266 ± 0.008 d | 10.02 ± 0.49 d |
| PorphSR_CMC_Gly | 0.089 ± 0001 | 0.21 ± 0.42 | 0.180 ± 0.016 c | 7.09 ± 0.84 c |
| PorphSR_AL | 0.095 ± 0.011 | −0.41 ± 0.41 | 0.106 ± 0.014 e | 6.84 ± 1.54 c |
| PorphSR_AL_Gly | 0.094 ± 0.006 | −0.76 ± 0.62 | 0.113 ± 0.010 e | 5.36 ± 0.52 c |
| Negative Control | 0.099 ± 0.002 | 0.16 ± 0.94 | 0.048 ± 0.012 | 0.52 ± 0.49 |

### *3.3. Electron Microscopy*

Figure 2 shows surface features of the developed films.

### *3.4. Mechanical Tests*

The mechanical properties (Young's Modulus and UTS), determined by the described methods, are presented in Table 4.

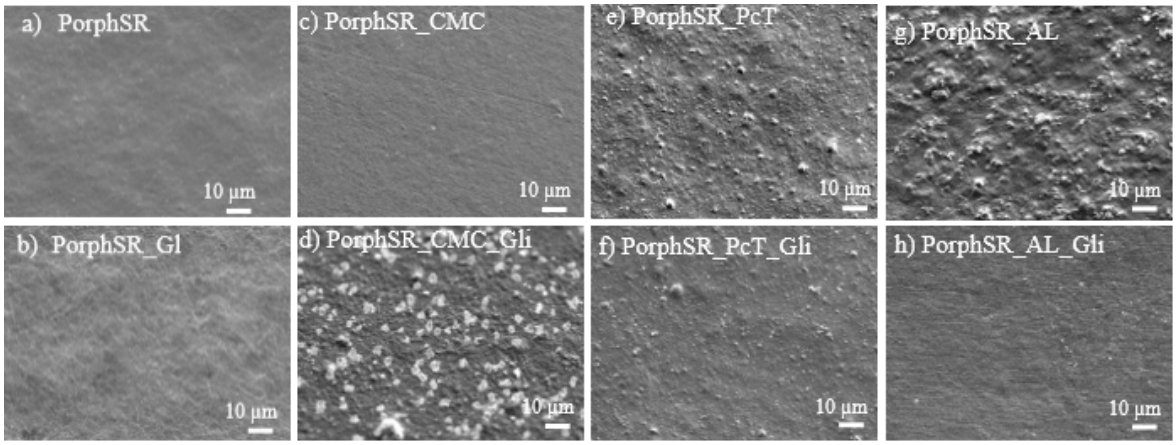


**Figure 2.** SEM images of the produced films: (**a**) PorphSR, (**b**) PorphSR_Gly, (**c**) PorphSR_CMC, (**d**) PorphSR_CMC_Gly, (**e**) PorphSR_PcT, (**f**) PorphSR_PcT_Gly, (**g**) PorphSR_AL, (**h**) PorphSR_AL_Gly.

**Table 4.** Young's Modulus and Ultimate Tensile Stress average values obtained for the produced films. Lowercase letters on data symbolize the statistically significant differences with a significance of 5%.

| | **Young's Modulus (MPa)** | **UTS (MPa)** |
|---|---|---|
| PorphSR_ | 2897.23 ± 524.44 | 12.86 ± 0.79 a |
| PorphSR_Gly | 1122.20 ± 200.54 a | 4.34 ± 0.78 b |
| PorphSR_PcT | 3992.34 ± 272.28 b | 26.00 ± 5.92 c |
| PorphSR_PcT_Gly | 1629.00 ± 142.41 a | 23.18 ± 1.62 c |
| PorphSR_CMC | 1624.15 ± 330.61 a | 10.26 ± 2.57 ab |
| PorphSR_CMC_Gly | 1648.12 ± 297.32 a | 21.94 ± 4.28 ac |
| PorphSR_AL | 4209.78 ± 191.25 b | 17.36 ± 4.96 abc |
| PorphSR_AL_Gly | 1576.02 ± 424.38 a | 9.33 ± 3.00 abc |

### *3.5. Sensory Analysis*

Figure 3 shows the chocolate cereal balls packed with different films, namely PorphSR_CMC_Gly, PorphSR_PcT_Gly, PorphSR_AL_Gly and polyethylene (control). The data obtained was analyzed according to Meilgaard et al. (1999) [50]. Figure 4 represents, on the left, the number of correct answers in the identification of the different chocolate cereal ball originating from packages made with the produced films (different films between themselves) and, on the right, the number of correct answers in the identification of the different chocolate cereal ball originating from packages made with the produced films and the control (different films against the control), as well as the critical number of correct answers in the black column, which represents the number of correct answers from which the existence of perception of difference is identified with a significance of 5%.

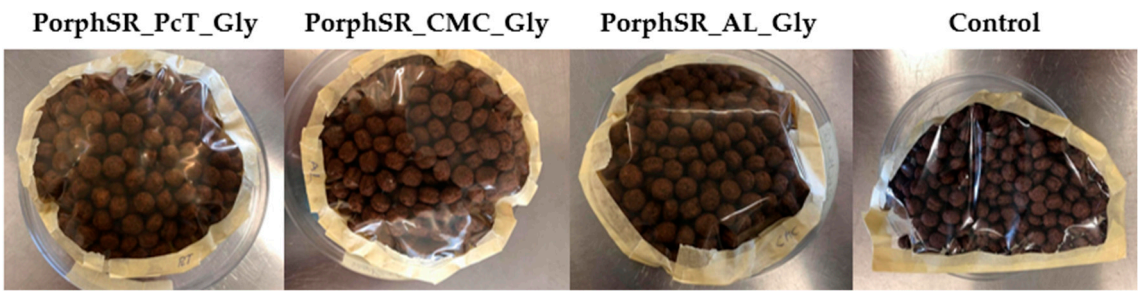


**Figure 3.** Cereals with chocolate packaged in packaging produced from PorphSR_PcT_Gly, PorphSR_CMC_Gly and PorphSR_CMC_Gly and Polyethylene (Control) films.

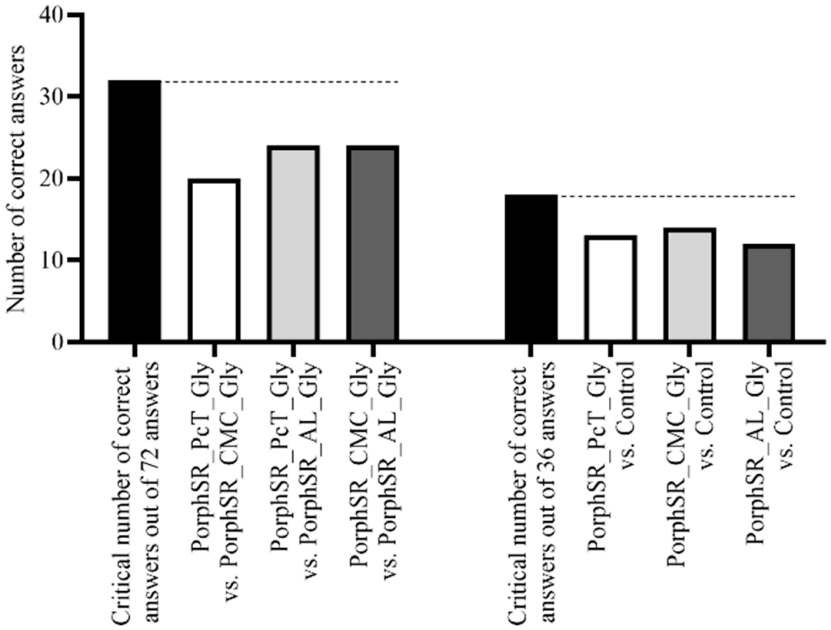


**Figure 4.** Number of correct answers in the differentiation through sensory analysis of cereal balls with chocolate packaged in PorphSR_PcT_Gly, PorphSR_CMC_Gly, PorphSR_CMC_Gly) and in polyethylene (control) films.

## 4. Discussion

### *4.1. Extraction Methods*

The PorphSR yield obtained by the present process is very high, at 26.66%, as presented in Table 2, especially compared to other known methods with yields that vary from 6.24 to 17.6% of the initial dry weight [41,51,52]. The procedure for the extraction of PorphSR is reproducible, as the differences in yields, concentration of D-galactose and total phenols in the samples (Table 2) are not statistically significant.

Although the extraction process is reproducible, the extract has some contaminants. The presence of these substances in semi-refined porphyran extracts is due to the association of several compounds with porphyran molecules that make up the structure of the cell wall, as it has a complex and heterogeneous structure [29]. The presence of phenols was detected at a level of 0.616 equivalents of gallic acid $\mu g \cdot mg^{-1}$ of extract, however, the method used, QTP with Folin–Ciocalteu reagent, despite being widely used, is based on the oxidation of compounds with sufficient reducing character, thus not being a detection reaction unique to phenols and opening up the possibility of interference from other compounds [53]. The samples show a negligible degree of protein contamination, and when compared with the extraction procedure described by He et al., 2019, with a protein concentration between 1.1–0.4%, are lower. The D-galactose concentration of 67.74% in dry weight is close to the expected for pure porphyran [54], since this is the monomer of the porphyran structure (residues (1,3-β) D-galactose alternating with (1,4-α) L-galactose-6-sulfate or 3,6-anhydro-α-L-galactose) [40].

### *4.2. Antioxidant Potential*

In the analysis of antioxidant activity of the polysaccharide extract, it was necessary to take into consideration the antioxidant activity against various types of oxidants, from reactive oxygen species (ROS) generated from hydrogen peroxide to milder single-electron oxidants such as the DPPH and ABTS radicals [55]. Alcohols and phenols can exhibit radical scavenging activity, with phenols being typically more effective reducing agents than aliphatic alcohols, thus being reactive towards milder oxidants such as DPPH and ABTS radicals [56]. Porphyran, being a polysaccharide, was expected to present some degree of antioxidant activity, on account of the alcohol groups that are part of the polymeric

structure. The extent of the antioxidant activity of the porphyrans described herein was assessed by HPSA, DPPH, FRAP and ABTS methods (Table 3).

Some carbohydrates, such as carrageenan [57] and glucose [58], have antioxidant potential against ROS of $H_2O_2$ origin. Regarding the tested porphyrans, it was observed that PorphSR, shows antioxidant potential when compared to the control. As mentioned earlier, this antioxidant activity can be assigned to the presence of alcohol functional groups on the polysaccharide structure and is analogous to the radical scavenging activity exhibited by simple alcohols [59]. The antioxidant action can be the result from the transfer of $H^+$ cations to OH• or the uptake of $O_2^-$• [60]. These are the main oxidation promoting species in organisms and greatly impact their health.

#### 4.2.1. Hydrogen Peroxide Scavenging Assay (HPSA)

In HPSA, antioxidant activities were observed in PorphSR extract (Δ 0.066), in PcT (Δ 0.019), in Gly (Δ 0.028) and PorphSR_PcT (Δ 0.017) and PorphSR_PcT_Gly (Δ 0.028) films, with PcT showing the highest activity. The components CMC (Δ 0.108) and AL (Δ 0.113) did not promote oxidation. The remainder showed no statistically significant differences from the control.

In the HPSA assays, it was observed that PorphSR, pectin and glycerol presented some antioxidant activity against ROS generated from the NaFeEDTA-promoted decomposition of $H_2O_2$ when compared to the control reaction [61]. In the case of pectin, the antioxidant activity against ROS was superior to that of glycerol and porphyran; however, it should be noted that the pectin used was food grade, and it also contained glucose, sodium acid pyrophosphate and tricalcium phosphate, which can contribute to the overall radical scavenging potential [55]. In the case of sodium carboxymethylcellulose, sodium alginate and the respective composites with porphyran, oxidation was only slightly suppressed or even promoted. This was probably due to alkaline carboxylate groups that promote the deprotonation of hydrogen peroxide, increasing the formation of $HOO^-$, resulting in an increased prevalence on uncontrolled Fenton reactions [62,63].

#### 4.2.2. DPPH (2,2-Diphenyl-1-Picrylhydrazyl) Radical Scavenging Activity

In the DPPH method, the PorphSR extract showed antioxidant potential (2.23%). The remaining components and the films did not show statistically significant differences from the control.

#### 4.2.3. Ferric-Reducing Antioxidant Power (FRAP)

In the FRAP method, once again the PorphSR extract showed the more promising antioxidant potential (0.420 ascorbic acid equivalent $\mu g \cdot mg^{-1}$ of sample), and the remaining components did not show antioxidant potential. However, all the films, PorphSR_PcT, PorphSR_PcT_Gly, PorphSR_CMC, PorphSR_CMC_Gly, PorphSR_AL and PorphSR_AL_Gly (0.207, 0.168, 0.266, 0.180, 0.106 and 0.113 ascorbic acid equivalent $\mu g \cdot mg^{-1}$ of sample, respectively), showed antioxidant potential, especially the film PorphSR_CMC.

#### 4.2.4. 2,2′-Azinobis-(3-Ethylbenzothiazoline-6-Sulfonic Acid Assay (ABTS)

Tests with the ABTS method showed similar results to the FRAP method. Amongst the film components, only PorphSR extract (20.46%) showed antioxidant potential, and among the films PorphSR_PcT, PorphSR_PcT_Gly, PorphSR_CMC, PorphSR_CMC_Gly, PorphSR_AL and PorphSR_AL_Gly (7.51%, 6.62%, 10.02%, 7.09%, 6.84% and 5.36%, respectively), all demonstrated antioxidant potential.

#### 4.2.5. Comparative Analysis of the Different Assays

In the DPPH, FRAP and ABTS tests, the only component that shows statistically significant differences, with a significance of 5% for the control, is porphyran, with a *p*-value less than 0.0001 in all tests. The other components (glycerol, CMC, sodium alginate and pectin) did not show discernible activity. The antioxidant potential of semi-refined porphyran

stands out due to its observed antioxidant activity against DPPH, ABTS and the FRAP reagent. This bioactivity was not expected on sulfated polysaccharides such as porphyran, justifiable most probably by the presence of phenols and other secondary metabolites capable of undergoing single-electron transfer reactions [55]. Porphyran extracts are reported to have low antioxidant activity in one-electron donation assays such as DPPH, with less than a 2% inhibition rate at similar concentrations [64] and in ABTS an inhibition rate in the range of 1.5–2.8% [65]. Only in aqueous extracts with a high content of phenols was this activity found to be higher [66]. Thus, it is most likely that this action does not derive from porphyran itself but from other reducing molecules likely to be present in the extract, as porphyran has a complex and heterogeneous structure [29], as also noted above and as noted in the total quantification of phenols (Table 2).

Another important point to emphasize is the importance of applying different tests to determine the antioxidant potential in order to account for all the different oxidation mechanisms occurring in each assay, the reaction stoichiometry, the reaction rate (DPPH and FRAP are slower than ABTS) and the method resolution (DPPH in different solvents). Therefore, by combining the different methods, a more complete antioxidant profile is obtained [67].

In accordance with the assays carried out with individual components, the films containing porphyran and pectin showed high antioxidant potential in HPSA.

The films prepared with CMC and AL exhibited antioxidant activities similar to the control reaction, which is consistent with the pro-oxidant activity of CMC and AL, mentioned earlier. The presence of glycerol had a negligible effect on the overall antioxidant activity. In DPPH scavenging assay, all samples presented low to no antioxidant activity. This contrasts with the activities observed in HPSA for porphyran, pectin and glycerol. There were no statistically significant differences between the control and the films PorphSR_PcT, PorphSR_PcT_Gly, PorphSR_CMC, PorphSR_CMC_Gly, PorphSR_AL and PorphSR_AL_Gly, in terms of DPPH scavenging activity. The low scavenging activity towards DPPH can be explained by the low reactivity of aliphatic alcohols towards this stable radical. For instance, methanol is a commonly used solvent in this type of assay. Since porphyran, Al, CMC and glycerol are also structurally alcohols, their lack of DPPH scavenging activity appears consistent with that exhibited by simpler alcohols.

The FRAP method demonstrates that the activity of the films is proportional to their PorphSR composition, with the films PorphSR_PcT, PorphSR_PcT_Gly and PorphSR_CMC_Gly showing roughly half the activity of PorphSR, $0.207 \pm 0.028$; $0.168 \pm 0.049$; $0.180 \pm 0.016$ and $0.420 \pm 0.014$, respectively, and PorphSR_AL and PorphSR_AL_Gly roughly a quarter, at $0.106 \pm 0.014$ and $0.113 \pm 0.010$, respectively. In the ABTS test, the trend of proportionality with the concentration of PorphSR ($20.46 \pm 0.90$) observed in the FRAP test is maintained, with the PorphSR_PcT, PorphSR_PcT_Gly and PorphSR_CMC_Gly films ($7.51 \pm 1.31\%$; $6.62 \pm 0.41\%$ and $7.09 \pm 0.84\%$, respectively), whereas for the PorphSR_CMC film it is roughly half ($10.02 \pm 0.49\%$) and for the PorphSR_AL films and PorphSR_AL_Gly roughly a quarter ($6.84 \pm 1.54$ and $5.36 \pm 0.52$, respectively).

It was observed that, in general, the films containing porphyran extract presented some antioxidant activity, although the composites presented a noticeably lower activity, most likely due to the lower porphyran content. Nevertheless, the antioxidant activity presented by PorphSR against ROS, ABTS and Fe(III), is sufficiently high so that composite films with a broad antioxidant activity could be successfully prepared.

### *4.3. Electron Microscopy*

Porphyran films without added polysarides–PorphSR (Figure 2a) and PorphSR_Gly (Figure 2b) display a uniform microstructure and an apparently smoother surface. Observation at higher magnification shows that in the presence of glycerol the resulting structure consists in overlapping layers (Figure 2a). This probably results from differential drying shrinkage, caused by insufficient water in the matrix [68]. The addition of CMC to the semi-refined porphyran extract produces a uniform smooth film (Figure 2c). However, PorphSR_CMC_Gly displays biphasic microstructure (Figure 2d). The presence of a second

phase is commonly associated with linear polymers: the simple and relatively short chains are able to wind, forming ordered crystallites in the amorphous martrix. This was possibly triggered by repulsion interactions with glycerol molecules [69]. Among the films without glycerol, PorphSR_PcT (Figure 2e) and PorphSR_AL (Figure 2g) appear to display a higher surface roughness. This probably results from gas bubbles entrapped during drying of the high viscosity film-forming solutions. Scratches and small bubbles in PorphSR_CMC (Figure 2c), PorphSR_AL (Figure 2g) and PorphSR (Figure 2a) films are probably due to irregularities in the moulds and to presence of small trapped gas bubbles, respectively.

### *4.4. Mechanical Tests*

The mechanical properties, summarized in Table 4, show that adding glycerol to the films compositions leads to a Young's modulus decrease. PorphSR_Gly, PorphSR_PcT_Gly and PorphSR_AL_Gly films show a 61 ± 2% Young's Modulus reduction when compared with their counterparts, without added glycerol. Porphyran films without added polysarides (PorphSR) also displayed a reduced Young's Modulus (minus 29 ± 3%) when compared with the PorphSR_PcT and PorphSR_AL films.

Regarding films' tensile strength, no statistically significant differences were found between ProphSR_Pct and ProphSR_AL films with or without glycerol. Therefore, glycerol, while reducing the films' Young's Modulus, will not affect their tensile strength significantly. As an exception to this behavior, glycerol effectively reduced the PorphSR film tensile strength and Young's Modulus. Without the addition of other polysarides, ProphSR_Gly film tensile strength decreased to 4.34 ± 0.78 MPa, possibly due to large distance between chains [70].

Table 4 also shows no differences between PorphSR_CMC and PorphSR_CMC_Gly films Young's Modulus and a significant reduction of the PorphSR_CMC film tensile strength. As seen in Figure 2d, a biphasic microstructure points to an absent interaction between glycerol and CMC. PorphSR_CMC films might then be unable to provide the necessary interactions between matrix components, reducing their mechanical properties [71].

These results show that both semi-refined porphyran and glycerol can be used to reduce the films Young's Modulus while affecting the UTS. They contribute to ramified structures, where interactions (hydrogen bonds, electrostatic and van der Waals interactions) between matrix components increase tensile strength and elasticity [72–74].

Overall, the PorphSR_PcT_Gly film provided the best mechanical properties, with the Young's Modulus and the UTS reaching 1629.00 ± 142.41 and 26.00 ± 5.92 MPa, respectively.

### *4.5. Sensory Analysis*

The analysis of the results was based on Meilgaard et al. (1999), in which a number of correct answers were established according to the number of total answers so that sensory differences could be considered as detected by the taster (critical number of correct answers), since there was not, in any of the cases studied, Figure 4, a number of correct answers greater than the critical number, it was considered that there was no detection of sensory differences between the cereals packed with any of the films developed between them and between the control. Thus, after 2 months, there is no perceptible difference, neither between the films among themselves, nor in the comparison of films with the control. The chocolate cereal balls maintain crispness and show no change in flavor indicating that lipid oxidation is minimal, which may be due either to the antioxidant activity of the films or the barrier effect of the film. The crispness of cereals after two months also allows us to conclude that the permeability of films to water vapor is low.

Based on these preliminary tests we can infer that the developed films have the potential to replace polyethylene in the packaging of chocolate cereals; however, further testing is needed in order to determine maximum shelf-life, as well as repeat the sensory trials with a larger group of trained tasters, increasing the representativeness of the results.

## 5. Conclusions

PorphSR extraction is a method that allows the extraction of semi-refined porphyran from an abundant and easy-to-grow algae, *Porphyra dioica*, using a green solvent, hot water, with a high yield of 26.66%, a 67.74% galactose content and undetectable protein contamination. Additionally, the extraction procedure is reproducible and shows scale-up potential. It presents itself as an efficient and low-polluting extraction method from available and renewable raw materials. In the development of the films, the same principle was applied, establishing a process that uses only thermal energy in its preparation, with no application of a cross-linking agent, keeping the filmogenic solution as minimally complex as possible, resulting in the resistance of these films to moisture and broadening its scope of application. The main films developed, PorphSR_CMC_Gly, PorphSR_PcT_Gly and PorphSR_AL_Gly, showed good durability over the time they were analyzed (2 months), maintaining their chemical and physical properties, even when subject to changing atmospheric conditions. The film with the best performance was PorphSR_PcT_Gly, because its bioactivities were equivalent (DPPH, ABTS and FRAP) or higher (HPSA) than other filmogenic solutions. This film also displayed the best mechanical performance, combining the highest tensile strength with a low Young's modulus. The sensory analysis showed that the films developed based on porphyran have the potential to be used in the packaging of dry foods with a high lipid content. In order to consider these films as substitutes for common plastics in food packaging, it is necessary to carry out more tests, such as migration tests, determination of the water vapor permeability rate, $O_2$ and $CO_2$ permeability rates, and extend the mechanical characterization.

**Author Contributions:** Conceptualization, M.T., P.A., C.A., M.G. and S.B.; Data curation, M.T., P.A., C.A., R.B. (Raul Bernardino), M.G., R.B. (Ricardo Baptista) and S.B.; Formal analysis, M.T., P.A., C.A., R.B. (Raul Bernardino), M.G., R.B. (Ricardo Baptista) and S.B.; Funding acquisition, C.A., R.B. (Raul Bernardino), M.G., R.B. (Ricardo Baptista) and S.B.; Investigation, M.T., P.A., C.A., R.B. (Raul Bernardino), M.G., R.B. (Ricardo Baptista); Methodology, M.T., P.A., C.A., M.G. and R.B. (Ricardo Baptista); Project administration, C.A., R.B. (Raul Bernardino) and S.B.; Resources, C.A., R.B. (Raul Bernardino), M.G., R.B. (Ricardo Baptista) and S.B.; Software, R.B. (Ricardo Baptista); Supervision, C.A. and S.B.; Validation, M.T., P.A., C.A., R.B. (Raul Bernardino), M.G., R.B. (Ricardo Baptista) and S.B.; Visualization, M.T., P.A., C.A., R.B. (Raul Bernardino), M.G., R.B. (Ricardo Baptista) and S.B.; Writing—original draft, M.T.; Writing—review & editing, M.T., P.A., C.A., R.B. (Raul Bernardino), M.G., R.B. (Ricardo Baptista) and S.B. All authors have read and agreed to the published version of the manuscript.

**Funding:** This research was funded by Fundação para a Ciência e Tecnologia (FCT) through the strategic project UIDB/04292/2020 granted to MARE. Raul Bernardino acknowledges to Base-UIDB/50020/2020 and Programmatic-UIDP/50020/2020 Funding of LSRE-LCM, funded by national funds through FCT/MCTES (PIDDAC). Mafalda Guedes acknowledges FCT funding under CeFEMA contract UIDB/04540/2020 and Ricardo Baptista acknowledges FCT through IDMEC under LAETA, project UIDB/50022/2020.

**Institutional Review Board Statement:** Not applicable.

**Informed Consent Statement:** Not applicable.

**Data Availability Statement:** The data presented in this study are available on request from the corresponding author [C.A.] upon reasonable request.

**Acknowledgments:** The authors thank the Lisbon Biomechanics Laboratory for the films' tensile stress tests.

**Conflicts of Interest:** The authors declare no conflict of interest.

## References


1. Yeo, B.G.; Takada, H.; Hosoda, J.; Kondo, A.; Yamashita, R.; Saha, M.; Maes, T. Polycyclic aromatic hydrocarbons (PAHs) and hopanes in plastic resin pellets as markers of oil pollution via international pellet watch monitoring. *Arch. Environ. Contam. Toxicol.* **2017**, *73*, 196–206. [CrossRef] [PubMed]
2. Urbanek, A.K.; Rymowicz, W.; Mirończuk, A.M. Degradation of plastics and plastic-degrading bacteria in cold marine habitats. *Appl. Microbiol. Biotechnol.* **2018**, *102*, 7669–7678. [CrossRef] [PubMed]
3. McKinsey, E.M.F. *The New Plastics Economy—Rethinking the Future of Plastics*; Routledge: London, UK, 2016.
4. Plastics Europe. *Plastics—The Facts 2020*; Plastics Europe: Brussels, Belgium, 2020.
5. Derraik, J.G. The pollution of the marine environment by plastic debris: A review. *Mar. Pollut. Bull.* **2002**, *44*, 842–852. [CrossRef]
6. Balestri, E.; Menicagli, V.; Vallerini, F.; Lardicci, C. Biodegradable plastic bags on the seafloor: A future threat for seagrass meadows? *Sci. Total Environ.* **2017**, *605–606*, 755–763. [CrossRef] [PubMed]
7. Mucientes, G.; Queiroz, N. Presence of plastic debris and retained fishing hooks in oceanic sharks. *Mar. Pollut. Bull.* **2019**, *143*, 6–11. [CrossRef] [PubMed]
8. Farrell, P.; Nelson, K. Trophic level transfer of microplastic: *Mytilus edulis* (L.) to *Carcinus maenas* (L.). *Environ. Pollut.* **2013**, *177*, 1–3. [CrossRef]
9. Feng, Z.; Zhang, T.; Wang, J.; Huang, W.; Wang, R.; Xu, J.; Fu, G.; Gao, G. Spatio-temporal features of microplastics pollution in macroalgae growing in an important mariculture area, China. *Sci. Total Environ.* **2020**, *719*, 137490. [CrossRef]
10. Alimba, C.G.; Faggio, C. Microplastics in the marine environment: Current trends in environmental pollution and mechanisms of toxicological profile. *Environ. Toxicol. Pharmacol.* **2019**, *68*, 61–74. [CrossRef]
11. Van Cauwenberghe, L.; Janssen, C.R. Microplastics in bivalves cultured for human consumption. *Environ. Pollut.* **2014**, *193*, 65–70. [CrossRef]
12. Wright, S.L.; Kelly, F.J. Plastic and human health: A micro issue? *Environ. Sci. Technol.* **2017**, *51*, 6634–6647. [CrossRef]
13. Iwata, T. Biodegradable and bio-based polymers: Future prospects of eco-friendly plastics. *Angew. Chem. Int. Ed.* **2015**, *54*, 3210–3215. [CrossRef] [PubMed]
14. Shen, M.; Song, B.; Zeng, G.; Zhang, Y.; Huang, W.; Wen, X.; Tang, W. Are biodegradable plastics a promising solution to solve the global plastic pollution? *Environ. Pollut.* **2020**, *263*, 114469. [CrossRef] [PubMed]
15. Pinheiro, A.C.; Cerqueira, M.A.; Souza, B.W.; Martins, J.T.; Teixeira, J.A.; Vicente, A.A. *Boletim de Biotecnologia*; Sociedade Portuguesa de Biotecnologia: Minho, Portugal, 2010; pp. 17–28.
16. Ramos, Ó.L.; Fernandes, J.C.; Silva, S.I.; Pintado, M.E.; Malcata, F.X. Edible films and coatings from whey proteins: A Review on formulation, and on mechanical and bioactive properties. *Crit. Rev. Food Sci. Nutr.* **2012**, *52*, 533–552. [CrossRef] [PubMed]
17. Ozen, B.F.; Floros, J.D. Effects of emerging food processing techniques on the packaging materials. *Trends Food Sci. Technol.* **2001**, *12*, 60–67. [CrossRef]
18. Marsh, K.; Bugusu, B. Food packaging-roles, materials, and environmental issues. *J. Food Sci.* **2007**, *72*, 39–55. [CrossRef]
19. Reboleira, J.; Adão, P.; Guerreiro, S.F.C.; Dias, J.R.; Ganhão, R.; Mendes, S.; Andrade, M.; Vilarinho, F.; Sanches-Silva, A.; Mateus, A.; et al. Poultry shelf-life enhancing potential of nanofibers and nanoparticles containing porphyra dioica extracts. *Coatings* **2020**, *10*, 315. [CrossRef]
20. Raheem, D. Application of plastics and paper as food packaging materials—An overview. *Emir. J. Food Agric.* **2013**, *25*, 177. [CrossRef]
21. Embuscado, M.E.; Hubber, K.C. Edible Films and Coatings: Why, What, and How? In *Edible Films and Coatings for Food Applications*; Huber, K.C., Embuscado, M.E., Eds.; Springer: New York, NY, USA, 2009; pp. 1–23.
22. Bolumar, T.; Andersen, M.L.; Orlien, V. Antioxidant active packaging for chicken meat processed by high pressure treatment. *Food Chem.* **2011**, *129*, 1406–1412. [CrossRef]
23. Khaneghah, A.M.; Hashemi, S.M.B.; Limbo, S. Antimicrobial agents and packaging systems in antimicrobial active food packaging: An overview of approaches and interactions. *Food Bioprod. Process.* **2018**, *111*, 1–19. [CrossRef]
24. Wang, H.; Qian, J.; Ding, F. Emerging chitosan-based films for food packaging applications. *J. Agric. Food Chem.* **2018**, *66*, 395–413. [CrossRef]
25. Wang, L.; Liu, Y.; Zhang, Z.; Wang, B.; Qiu, J.; Hui, D.; Wang, S. Polymer composites-based thermoelectric materials and devices. *Compos. Part B Eng.* **2017**, *122*, 145–155. [CrossRef]
26. Akhtar, H.M.S.; Riaz, A.; Hamed, Y.S.; Abdin, M.; Chen, G.; Wan, P.; Zeng, X. Production and characterization of CMC-based antioxidant and antimicrobial films enriched with chickpea hull polysaccharides. *Int. J. Biol. Macromol.* **2018**, *118*, 469–477. [CrossRef] [PubMed]
27. Roy, S.; Rhim, J.-W. Preparation of carbohydrate-based functional composite films incorporated with curcumin. *Food Hydrocoll.* **2020**, *98*, 105302. [CrossRef]
28. Fonseca, R.; Mourão, P. Fucosylated chondroitin sulfate as a new oral antithrombotic agent. *Thromb. Haemost.* **2006**, *96*, 822–829. [CrossRef] [PubMed]
29. Rahman, M. An Overview of the medical applications of marine skeletal matrix proteins. *Mar. Drugs* **2016**, *14*, 167. [CrossRef] [PubMed]
30. Caputo, H.E.; Straub, J.E.; Grinstaff, M.W. Design, synthesis, and biomedical applications of synthetic sulphated polysaccharides. *Chem. Soc. Rev.* **2019**, *48*, 2338–2365. [CrossRef] [PubMed]

31. Zaporozhets, T.; Besednova, N. Prospects for the therapeutic application of sulfated polysaccharides of brown algae in diseases of the cardiovascular system: Review. *Pharm. Biol.* **2016**, *54*, 3126–3135. [CrossRef]
32. Rocha, A.R. *Purificação e Caracterização dos Polissacarídeos da Água das Salinas de Aveiro*; Univercidade de Aveiro: Aveiro, Portugal, 2016.
33. Jiao, G.; Yu, G.; Zhang, J.; Ewart, H. Chemical structures and bioactivities of sulfated polysaccharides from marine algae. *Mar. Drugs* **2011**, *9*, 196–223. [CrossRef]
34. Klein, A.S.; Mathieson, A.C.; Neefus, C.D.; Cain, D.F.; Taylor, H.A.; Teasdale, B.W.; West, A.L.; Hehre, E.J.; Brodie, J.; Yarish, C.; et al. Identification of north-western Atlantic Porphyra (Bangiaceae, Bangiales) based on sequence variation in nuclear SSU and plastid *rbc*L genes. *Phycologia* **2003**, *42*, 109–122. [CrossRef]
35. Pereira, R.; Sousa-Pinto, I.; Yarish, C. Field and culture studies of the life history of Porphyra dioica (Bangiales, Rhodophyta) from Portugal. *Phycologia* **2004**, *43*, 756–767. [CrossRef]
36. Knoop, J.; Griffin, J.N.; Barrento, S. Cultivation of early life history stages of Porphyra dioica from the British Isles. *J. Appl. Phycol.* **2020**, *32*, 459–471. [CrossRef]
37. Pereira, R.; Yarish, C.; Sousa-Pinto, I. The influence of stocking density, light and temperature on the growth, production and nutrient removal capacity of Porphyra dioica (Bangiales, Rhodophyta). *Aquaculture* **2006**, *252*, 66–78. [CrossRef]
38. Roleda, M.Y.; Hurd, C.L. Seaweed nutrient physiology: Application of concepts to aquaculture and bioremediation. *Phycologia* **2019**, *58*, 552–562. [CrossRef]
39. Silva, D.M.; Valente, L.M.P.; Sousa-Pinto, I.; Pereira, R.; Pires, M.A.; Seixas, F.; Rema, P. Evaluation of IMTA-produced seaweeds (Gracilaria, Porphyra, and Ulva) as dietary ingredients in Nile tilapia, Oreochromis niloticus L., juveniles. Effects on growth performance and gut histology. *J. Appl. Phycol.* **2015**, *27*, 1671–1680. [CrossRef]
40. Fernando, I.P.S.; Kim, K.-N.; Kim, D.; Jeon, Y.-J. Algal polysaccharides: Potential bioactive substances for cosmeceutical applications. *Crit. Rev. Biotechnol.* **2019**, *39*, 99–113. [CrossRef] [PubMed]
41. Isaka, S.; Cho, K.; Nakazono, S.; Abu, R.; Ueno, M.; Kim, D.; Oda, T. Antioxidant and anti-inflammatory activities of porphyran isolated from discolored nori (*Porphyra yezoensis*). *Int. J. Biol. Macromol.* **2015**, *74*, 68–75. [CrossRef]
42. Amin, A.S.; El-Didamony, A.M. Colorimetric determination of benzocaine, lignocaine and procaine hydrochlorides in pure form and in pharmaceutical formulations using p-benzoquinone. *Anal. Sci.* **2003**, *19*, 1457–1459. [CrossRef]
43. Rao, P.; Pattabiraman, T.N. Reevaluation of the phenol-sulfuric acid reaction for the estimation of hexoses and pentoses. *Anal. Biochem.* **1989**, *181*, 18–22. [CrossRef]
44. Fu, L.; Xu, B.-T.; Xu, X.-R.; Qin, X.-S.; Gan, R.-Y.; Li, H.-B. Antioxidant capacities and total phenolic contents of 56 wild fruits from south china. *Molecules* **2010**, *15*, 8602–8617. [CrossRef]
45. Bektaşoğlu, B.; Özyürek, M.; Güçlü, K.; Apak, R. Hydroxyl radical detection with a salicylate probe using modified CUPRAC spectrophotometry and HPLC. *Talanta* **2008**, *77*, 90–97. [CrossRef]
46. Andrade, M.A.; Ribeiro-Santos, R.; Costa Bonito, M.C.; Saraiva, M.; Sanches-Silva, A. Characterization of rosemary and thyme extracts for incorporation into a whey protein based film. *LWT* **2018**, *92*, 497–508. [CrossRef]
47. Berker, K.I.; Güçlü, K.; Tor, I.; Apak, R. Comparative evaluation of Fe(III) reducing power-based antioxidant capacity assays in the presence of phenanthroline, batho-phenanthroline, tripyridyltriazine (FRAP), and ferricyanide reagents. *Talanta* **2007**, *72*, 1157–1165. [CrossRef] [PubMed]
48. Re, R.; Pellegrini, N.; Proteggente, A.; Pannala, A.; Yang, M.; Rice-Evans, C. Antioxidant activity applying an improved ABTS radical cation decolorization assay. *Free Radic. Biol. Med.* **1999**, *26*, 1231–1237. [CrossRef]
49. Nieto, M.B. Structure and Function of Polysaccharide Gum-Based Edible Films and Coatings. In *Edible Films and Coatings for Food Applications*; Embuscado, M.E., Huber, K.C., Eds.; Springer: New York, NY, USA, 2009; pp. 57–112.
50. Meilgaard, M.C.; Carr, B.T.; Civille, G.V. Overall difference tests: Does a sensory difference exist between samples? In *Sensory Evaluation Techniques*; Meilgaard, M.C., Carr, B.T., Civille, G.V., Eds.; Taylor & Francis: Boca Raton, FL, USA, 1999; pp. 56–95. ISBN 9781439832271.
51. He, D.; Wu, S.; Yan, L.; Zuo, J.; Cheng, Y.; Wang, H.; Liu, J.; Zhang, X.; Wu, M.; Choi, J.; et al. Antitumor bioactivity of porphyran extracted from Pyropia yezoensis Chonsoo2 on human cancer cell lines. *J. Sci. Food Agric.* **2019**, *99*, 6722–6730. [CrossRef] [PubMed]
52. Yu, X.; Zhou, C.; Yang, H.; Huang, X.; Ma, H.; Qin, X.; Hu, J. Effect of ultrasonic treatment on the degradation and inhibition cancer cell lines of polysaccharides from Porphyra yezoensis. *Carbohydr. Polym.* **2015**, *117*, 650–656. [CrossRef] [PubMed]
53. Ainsworth, E.A.; Gillespie, K.M. Estimation of total phenolic content and other oxidation substrates in plant tissues using Folin-Ciocalteu reagent. *Nat. Protoc.* **2007**, *2*, 875–877. [CrossRef] [PubMed]
54. Bojko, L.; de Jonge, G.; Lima, D.; Lopes, L.C.; Viana, A.G.; Garcia, J.R.; Pessôa, C.A.; Wohnrath, K.; Inaba, J. Porphyran-capped silver nanoparticles as a promising antibacterial agent and electrode modifier for 5-fluorouracil electroanalysis. *Carbohydr. Res.* **2020**, *498*, 108193. [CrossRef]
55. Gijsman, P. Polymer Stabilization. In *Handbook of Environmental Degradation of Materials*; Elsevier: Amsterdam, The Netherlands, 2012; pp. 673–714. ISBN 9781437734560.
56. Rong, S.; Sun, Y. Degradation of TAIC by water falling film dielectric barrier discharge—Influence of radical scavengers. *J. Hazard. Mater.* **2015**, *287*, 317–324. [CrossRef]

57. Yuan, H.; Song, J.; Zhang, W.; Li, X.; Li, N.; Gao, X. Antioxidant activity and cytoprotective effect of κ-carrageenan oligosaccharides and their different derivatives. *Bioorg. Med. Chem. Lett.* **2006**, *16*, 1329–1334. [CrossRef]
58. Cherkas, A.; Holota, S.; Mdzinarashvili, T.; Gabbianelli, R.; Zarkovic, N. Glucose as a Major Antioxidant: When, What for and Why It Fails? *Antioxidants* **2020**, *9*, 140. [CrossRef]
59. McDonough, K. Antioxidant nutrients and alcohol. *Toxicology* **2003**, *189*, 89–97. [CrossRef]
60. Wan, A.; Xu, Q.; Sun, Y.; Li, H. Antioxidant Activity of High Molecular Weight Chitosan and N,O-Quaternized Chitosans. *J. Agric. Food Chem.* **2013**, *61*, 6921–6928. [CrossRef] [PubMed]
61. Ayude, M.A.; Doumic, L.I.; Cassanello, M.C.; Nigam, K.D.P. Clean catalytic oxidation for derivatization of key biobased platform chemicals: Ethanol, glycerol, and hydroxymethyl furfural. *Ind. Eng. Chem. Res.* **2019**, *58*, 16077–16095. [CrossRef]
62. Jeon, H.; Hong, S. Peroxide bond cleavage of nonheme iron-(hydro/alkyl)peroxo complexes induced by endogenous and exogenous factors. *Chem. Lett.* **2019**, *48*, 80–85. [CrossRef]
63. Mas-Ballesté, R.; Que, L. Iron-catalyzed olefin epoxidation in the presence of acetic acid: Insights into the nature of the metal-based oxidant. *J. Am. Chem. Soc.* **2007**, *129*, 15964–15972. [CrossRef]
64. Chen, X.-W.; Huang, W.-B.; Sun, X.-Y.; Xiong, P.; Ouyang, J.-M. Antioxidant activity of sulfated Porphyra yezoensis polysaccharides and their regulating effect on calcium oxalate crystal growth. *Mater. Sci. Eng. C* **2021**, *128*, 112338. [CrossRef]
65. Adão, P.; Reboleira, J.; Teles, M.; Santos, B.; Ribeiro, N.; Teixeira, C.M.; Guedes, M.; Pessoa, J.C.; Bernardino, S. Enhancement of the antioxidant and antimicrobial activities of porphyran through chemical modification with tyrosine derivatives. *Molecules* **2021**, *26*, 2916. [CrossRef]
66. Bhatia, S.; Sardana, S.; Senwar, K.R.; Dhillon, A.; Sharma, A.; Naved, T. In vitro antioxidant and antinociceptive properties of *Porphyra vietnamensis*. *BioMedicine* **2019**, *9*, 3. [CrossRef]
67. Apak, R. Current issues in antioxidant measurement. *J. Agric. Food Chem.* **2019**, *67*, 9187–9202. [CrossRef]
68. Han, J.H.; Aristippos, G. Edible Films and Coatings: A review. In *Innovations in Food Packaging*; Elsevier: Amsterdam, The Netherlands, 2005; Volume 15, pp. 239–262. ISBN 0-12-311632-5.
69. Wu, D.; Chang, P.R.; Ma, X. Preparation and properties of layered double hydroxide–carboxymethylcellulose sodium/glycerol plasticized starch nanocomposites. *Carbohydr. Polym.* **2011**, *86*, 877–882. [CrossRef]
70. Cian, R.E.; Salgado, P.R.; Drago, S.R.; Mauri, A.N. Effect of glycerol and $Ca^{+2}$ addition on physicochemical properties of edible carrageenan/porphyran-based films obtained from the red alga, Pyropia columbina. *J. Appl. Phycol.* **2015**, *27*, 1699–1708. [CrossRef]
71. Han, Y.; Yu, M.; Wang, L. Physical and antimicrobial properties of sodium alginate/carboxymethyl cellulose films incorporated with cinnamon essential oil. *Food Packag. Shelf Life* **2018**, *15*, 35–42. [CrossRef]
72. Espitia, P.J.P.; Du, W.-X.; Avena-Bustillos, R.d.J.; Soares, N.d.F.F.; McHugh, T.H. Edible films from pectin: Physical-mechanical and antimicrobial properties—A review. *Food Hydrocoll.* **2014**, *35*, 287–296. [CrossRef]
73. Meng, F.; Zhang, Y.; Xiong, Z.; Wang, G.; Li, F.; Zhang, L. Mechanical, hydrophobic and thermal properties of an organic-inorganic hybrid carrageenan-polyvinyl alcohol composite film. *Compos. Part B Eng.* **2018**, *143*, 1–8. [CrossRef]
74. Zhang, F.; Meng, F.; Wang, Z.Y.; NA, W. Interpolymer complexation between copovidone and carbopol and its effect on drug release from matrix tablets. *Drug Dev. Ind. Pharm.* **2017**, *43*, 190–203. [CrossRef] [PubMed]